Simulation study of neutrino nucleus cross section measurement in a segmented detector at a spallation neutron source*

YANG Zhen-Wei(杨振伟)[1,2,3;1)] DING Ming-Ming(丁明明)[1,2,3] CHEN Shao-Min(陈少敏)[1,2,3]
WANG Zhe(王喆)[3,4] ZHANG Feng(张锋)[1,2,3] GAO Yuan-Ning(高原宁)[1,2,3]

[1] Key Laboratory of Particle & Radiation Imaging (Tsinghua University), Ministry of Education, Beijing 100084, China
[2] Department of Engineering Physics, Tsinghua University, Beijing 100084, China
[3] Center for High Energy Physics, Tsinghua University, Beijing 100084, China
[4] Physics Department, Brookhaven National Laboratory, USA

Abstract: Knowledge of ν_e-Fe/Pb differential cross sections for ν_e energy below several tens of MeV scale is believed to be crucial in understanding supernova physics. In a segmented detector at a spallation neutron source, ν_e energy reconstructed from the electron range measurement is strongly affected because both multiple scattering and electromagnetic showers occur along the electron passage in target materials. In order to estimate these effects, a simulation study has been performed with a cube block model assuming perfect tracking precision. The energy spectrum distortion is observed to be proportional to the atomic number of the target material. Feasibility of unfolding the distorted ν_e energy spectrum is studied for both Fe and Pb. An evaluation of the statistical accuracy attainable is therefore provided for a segmented detector.

Key words: unfolding, neutrino, differential cross section, segmented detector, Monte Carlo, SNS, supernova

PACS: 29.30.Dn, 29.40.Wk, 95.55.Vj **DOI:** 10.1088/1674-1137/36/6/010

1 Introduction

Precise knowledge of the differential cross sections for quasi-elastic neutrino-nucleus scattering at a scale up to several tens of MeV is of importance in understanding the explosion dynamics of supernovae, since the neutrinos play a decisive role in the development between the prompt shock and the delayed shock [1]. Among the cross sections, neutrino interactions with ^{2}H, C, O, Fe and Pb are most relevant. In this low energy scale, the cross section varies rapidly, leading to large uncertainty in predicting core collapse supernovae[2, 3]. Although some theoretical calculations [4] of neutrino-nucleus cross sections have been performed in recent years, large uncertainties still exist and need to be clarified from experiments. On the experimental side, differential cross sections with C and O have been measured by the KARMEN and LSND experiments [5, 6], but those with Fe and Pb are still not available. In this paper, we present a simulation study of the cross section measurement of neutrino interaction with Fe and Pb. Our motivation was to provide an estimate of the achievable limit in neutrino cross section measurement experiments with a segmented detector at a spallation neutron source (SNS).

At an SNS, protons are driven to hit a target, producing a large amount of neutrons and by-product pions. The negative pions are mostly captured in the target, while the positive pions, after having been stopped in the target within 0.1 ns or so, undergo the characteristic successive decay scheme $\pi^+ \xrightarrow{26\ \mathrm{ns}} \mu^+ + \nu_\mu$ and followed by $\mu^+ \xrightarrow{2200\ \mathrm{ns}} e^+ + \nu_e + \bar{\nu}_\mu$. The resultant ν_e's can have a flux up to $2\times10^7/\mathrm{cm}^2/\mathrm{s}$ at a distance of 20 meters away from the spallation target at the SNS at Oak Ridge National Laboratory, assuming the SNS power to be 1 MW [7]. Since the time structure of the SNS beam provides a unique

Received 5 September 2011, Revised 11 October 2011
* Supported by National Natural Science Foundation of China (10875062, 10905033)
1) E-mail: yangzhw@tsinghua.edu.cn

advantage for neutrino studies [7–9], backgrounds are strongly suppressed. In the SNS target, the pions are stopped and decay to muons. The subsequent muon decay produces equal intensities of ν_e and $\bar{\nu}_\mu$, with a maximum energy 52.8 MeV. The energy spectra of the three kinds of neutrinos are shown in Fig. 1.

Such an energy range overlaps extremely well with that of supernova neutrinos. This characteristic makes it valuable to measure the cross sections of interactions between neutrinos and various target materials at an SNS. Fig. 2 shows the sketch of a neutrino detector at an SNS. A ν-SNS project [7] was proposed to build a neutrino facility at the SNS at the Oak Ridge National Laboratory. However, there is no report available detailing how precise the achievable measurements will be.

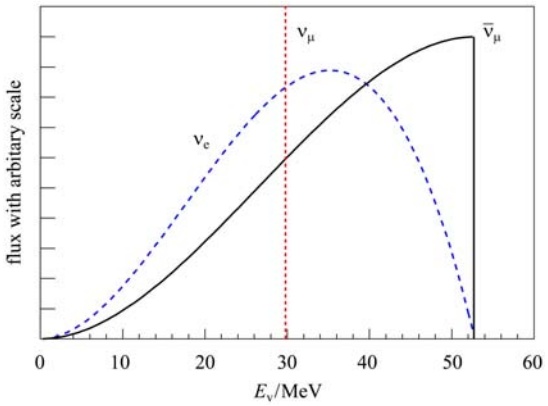

Fig. 1. Neutrino spectra from muon and pion decay-at-rest at a spallation neutron source.

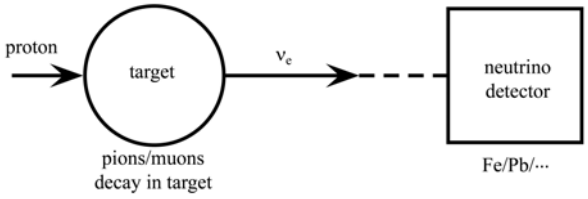

Fig. 2. Sketch of a neutrino detector at an SNS.

Electron neutrinos interacting with the target material at an SNS undergo both neutral- and charged-current interactions, while muon neutrinos can only undergo neutral-current interactions due to the limitation of kinematics. Neutral-current events are suppressed by at least two orders of magnitude in comparison with the charged-current events and can only be measured by the decay of excited nuclei. The charged-current events can be detected via the outgoing electron in the neutrino-nucleus reaction $\nu_e + {}^{A}_{Z}X_N \rightarrow {}^{A}_{Z+1}Y_{N-1} + e^-$ ($\nu_e + n \rightarrow p + e^-$). Since the neutrino energy is much lower than the nucleus, considering the charged-current quasi-elastic(CCQE) process and ignoring fermi motion of nucleus, the neutrino energy E_{ν_e} can be determined by the induced electron energy E_e,

$$E_{\nu_e} = E_e + \Delta, \tag{1}$$

where Δ is the mass difference between the final state nucleus Y and the initial state nucleus X. Therefore, a precise energy reconstruction of the ν_e induced electrons is essential for determining the differential cross sections. A segmented detector is proposed to measure the trajectories of ν_e induced electrons in the target. However, the energy loss of the electron is dominated by ionization at low energy, while above the critical energy E_c, it will be dominated by bremsstrahlung. The electromagnetic shower caused by bremsstrahlung will lead to a large uncertainty in measurements of the electron track length for energy above E_c. The critical energy can be approximated [10, 11] by E_c=800 MeV/(Z+1.2), where Z is the atomic number of the target nucleus. Therefore the critical energy of Fe is $E_c = 29.4$ MeV, and E_c=9.6 MeV for Pb. This makes it impossible to obtain the electron energy by its track length event by event. In this paper, we will show a statistical application to unfold the distorted energy spectrum, and leading to a reasonable resolution of the differential cross section.

The outline of this paper is as followed. In Section 2, the Geant 4 simulation of neutrino induced electrons are simulated in Fe and Pb. The simulation results and analysis are described in Section 3, and a brief conclusion is made in Section 4.

2 Simulation procedure

To simplify the issue, we use a cube block target material with a fiducial volume of 1 m×1 m×1 m, instead of a segmented detector with a target, tube, wire, etc. The tracking resolution is assumed to be perfect. The Geant 4 (version 9.0p01) package [12] is applied in this simulation study.

The cross section of neutrino-nucleus scattering is rather small, we therefore directly simulate the behaviors of the induced electron in the target. The electron input energy spectrum is the Michel distribution shaped by the theoretically predicted cross section given by R. Lazauskas and C. Volpe [4]. The maximum energy of induced electron, E_{max}, is approximately 48.2 MeV on ^{56}Fe, and the threshold energy of the interaction is $E_{thres} \simeq 5.1$ MeV. For ^{208}Pb, $E_{max} \simeq 49.9$ MeV, and $E_{thres} \simeq 3.4$ MeV.

Daughter products e.g., ^{56}Co, ^{208}Bi are ignored,

since the lifetimes of the daughters are long comparing the search window (~ 10 micro seconds).

The material of the detector is selected to be iron or lead with natural abundances, but not pure ^{56}Fe or ^{208}Pb. Therefore, the measured cross section is an average of mixture isotopes of iron or lead. This affects iron slightly since the natural abundance of ^{56}Fe is 91.754%. For lead, the natural abundances of ^{208}Pb, ^{207}Pb and ^{206}Pb are 52.4%, 22.1% and 24.1%, respectively, the effect of the mixture should be considered seriously in later studies.

The electromagnetic process is very important in the interaction of electrons in nuclear material. Processes of multiple scattering, low energy ionization, and low energy bremsstrahlung are added for electrons in the simulation.

To perform the unfolding procedure [13–16], two kinds of spectra of electrons are generated: 1) Michel distribution used to obtain the detector response matrix; 2) Michel distribution weighted with the cross section of corresponding ν_e-nucleus interaction. The second one is considered the true distribution to be reconstructed. For each event, the electron's energy (input) E and track length L in the target are recorded.

The number of events attainable in one nominal year (assuming 10^7 seconds) is estimated by considering the electron neutrino flux, the size of the detector and the average cross section of ν_e-nucleus scattering. The expected maximum cross section at 52.8 MeV for Fe is $\sigma_{\mathrm{Fe,max}} \simeq 1.2\times10^{-39}$ cm^2, and it gives that the average cross section over energy is about $0.3\sigma_{\mathrm{Fe,max}}$. For Pb, $\sigma_{\mathrm{Fe,max}} \simeq 1.3\times10^{-38}$ cm^2, and the average cross section over energy is about $0.4\sigma_{\mathrm{Pb,max}}$. Assuming that the effective target volume is 1 m^3, and the flux of ν_e's is 2×10^7 cm$^{-2}\cdot$s^{-1}, the number of events in one nominal year is estimated to be 6.1×10^3 for an Fe target, and 3.4×10^4 for a Pb target.

3 Unfolding method

In the energy measurement, due to the detector resolution, efficiency, and sometimes an intrinsic physical reason, the true value in bin i, will usually migrate into the measured energy bin j. In other words, the measured distribution is usually distorted by the detector response, or the detector response is folded to the true distribution, leading to the measured distribution. In many cases, the true distribution could be restored by applying correction factors to the measured distribution. This method fails, however, if the relation between the true value and the measured ones is highly nonlinear where the behavior of the detector response is poor.

Suppose the true distribution is X_{true}, and the measured one is Y_{obs}. If the effects of efficiency and background are ignored, they satisfy

$$Y_{\mathrm{obs}} = R\cdot X_{\mathrm{true}}, \tag{2}$$

where R is the response matrix or the migration matrix which describes the effects of the detector response. The basic idea of unfolding is that the effects of detector response could be removed or unfolded by the inverse of the response matrix, i.e., the estimator of the true distribution X is

$$\hat{X}_{\mathrm{true}} = R^{-1}\cdot Y_{\mathrm{obs}}. \tag{3}$$

However, although this is an unbiased estimator with the smallest variance, the physics is totally swept away by unphysical oscillation. Regularization is needed to remove the unphysical oscillation, which is actually a compromise between bias and unphysical oscillation, controlled by the choice of regularization parameter. There are several different regularisation schemes [13–16], for example, Tiknonov reularizaton, regularization based on entropy, Bayesian regularization, regularization based on Singular Value Decomposition(SVD), etc. The most basic point of all is that the true distribution is believed to be smooth but not oscillating rapidly. In this study, we used the TSVDUnfold class in ROOT package [17]. TSVDUnfold is a class in ROOT for unfolding based on SVD technique, it is part of RooUnfold, a ROOT unfolding framework, developed by Tim Adye, et al. [18].

In the SNS neutrino experiment, to measure the differential cross section of neutrino-nucleus scattering, the true value is the energy of incident electron, which is principally unknown and supposed to be binned in histogram E, the measured value is the electron track length in the target, binned in histogram L. The response matrix R can be obtained by Monte Carlo simulation as long as we have full knowledge of the detector. The discrete expression,

$$L_j = \sum_{i=1}^{n_{\mathrm{a}}} R_{ji}\cdot E_i \quad (j=1,\cdots,n_{\mathrm{b}}), \tag{4}$$

where E_i is the number of events in bin i of E, L_j is the number of events in bin j, n_{a} and n_{b} are the numbers of bins of E and L, respectively. The physical meaning of R_{ji} is the probability of an event in bin i of the true distribution to migrate into bin j of the measured distribution. Therefore, the response matrix is actually the normalized two-dimensional scattering plot of L and E.

4 Simulation results and analysis

In the simulation, the electron track length L is directly read from Geant 4 with no uncertainty. The response matrix of the detector with an iron target is shown in Fig. 3(a), and that of the detector with a lead target is shown in Fig. 3(b), corresponding to 200000 electrons with Michel distributed energy. If the matrix were diagonal, one could easily obtain the incident electron energy through track length event by event. However, these two plots show significant non-diagonal elements in the response matrices, and hence it is impossible to obtain directly the incident energy through track length. Especially, it is obvious

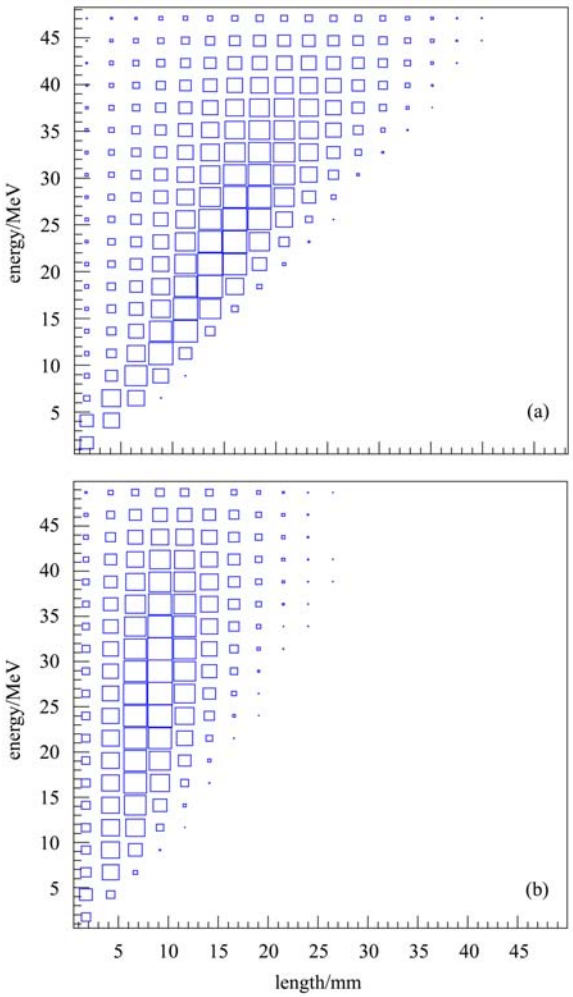

Fig. 3. Scattering plot of electron energy E versus track length L for target of Fe (a) and Pb (b). Significant non-diagonal elements of the response matrix exist due to an electromagnetic shower above critical energy E_c. The energy spectrum of incident electrons is the Michel distribution.

that the track length in an iron target is smeared widely with energy above 30 MeV, while for a lead target the smearing begins with energy above 10 MeV or so. This is the consequence of an electromagnetic shower. Both simulations are exactly consistent with the expected critical energies of Fe and Pb.

To extract the physical part of the unphysical oscillation, the choice of regularization parameter is crucial, which reflects a trade-off between bias and oscillation. For unfolding based on the SVD technique, the choice of regularization parameter should be tuned for a given distribution, number of bins and sample size. As described in Ref. [16], the regularization parameter kterm should be chosen by the plot of $\lg|d|_i$ versus i, where integer i is from 1 to the number of bins and the ith component of the vector d is the coefficient in the decomposition of the measured (and re-scaled) histogram. Only the first few terms, say k, of the decomposition should be significant for a reasonably smooth measured distribution, while the others correspond to the contribution of quickly oscillating basis vectors, and should be compatible with zero. Therefore, one should see two separate patterns on the plot of $\lg|d|_i$: for small i, $|d_i|$ is significantly greater than 1 and falls gradually to a standard gaussian distribution for large i. One should choose the regularization parameter kterm to be the critical value $i=k$, after which d_i's are insignificant.

Figure 4(a) shows the plot of $\lg|d_i|$ versus i with 5000 events accumulated in the Fe target; approximate data of one nominal year. The parameter kterm=5 is chosen from this plot. The unfolded energy spectrum of the ν_e induced electron is shown in the upper plot of Fig. 5(a), while the lower plot shows the discrepancy between the unfolded spectrum and the true one, where the latter is Michel distribution shaped by theoretical prediction of the differential cross section. With the unfolded energy spectrum of the induced electron, one can obtain the spectrum of the ν_e's that interact with the Fe target using Eq. (1). Dividing this spectrum by the Michel distribution gives the differential cross section of ν_e-nucleus scattering, as shown in the upper plot of Fig. 6(a). The lower plot in Fig. 6(a) shows the relative discrepancy between the measured cross section and the true one. One can see that the discrepancies and errors are huge for energy below 20 MeV, mainly because the low energy cross section is too small and few events are collected in this range. The discrepancy of the last bin is also large, around 30%. For other bins, the discrepancies are controlled within 20%. We checked this result by comparing it with five

other samples under the same condition. It shows that for energy below 20 MeV the measured cross sections fluctuate significantly, and are therefore totally unreliable. While the discrepancies between 20 and 50 MeV are well controlled within 20%. Increasing the sample size to be 10000 slightly improves the behavior between 20 and 50 MeV, but helps less (if at all) for the region below 20 MeV.

For a Pb target, the sample size is 30000. Fig. 4(b) shows the plot of $\lg|d_i|$ versus i, according to which, the regularization parameter kterm=4 is chosen for Pb. The unfolded energy spectrum of the ν_e induced electron is shown in the upper plot of Fig. 5(b), and the lower plot shows the discrepancy between the unfolded and true spectrum, where the true one is Michel distribution shaped by the theoretically predicted cross section of ν_e-Pb interaction. The resulting differential cross section of ν_e-Pb scattering is shown in the upper plot of Fig. 6(b), and the lower plot shows the relative discrepancy between the measured differential cross section and the true one. Similar to the case of an Fe target, one can see that the discrepancies and errors are large for energy below 22 MeV due to a lack of events. The discrepancy of the last bin is also large, around 30%. For other bins, energy between 25 and 50 MeV, the discrepancies are well controlled within 20%. This result is compared with five other samples using the same regularization

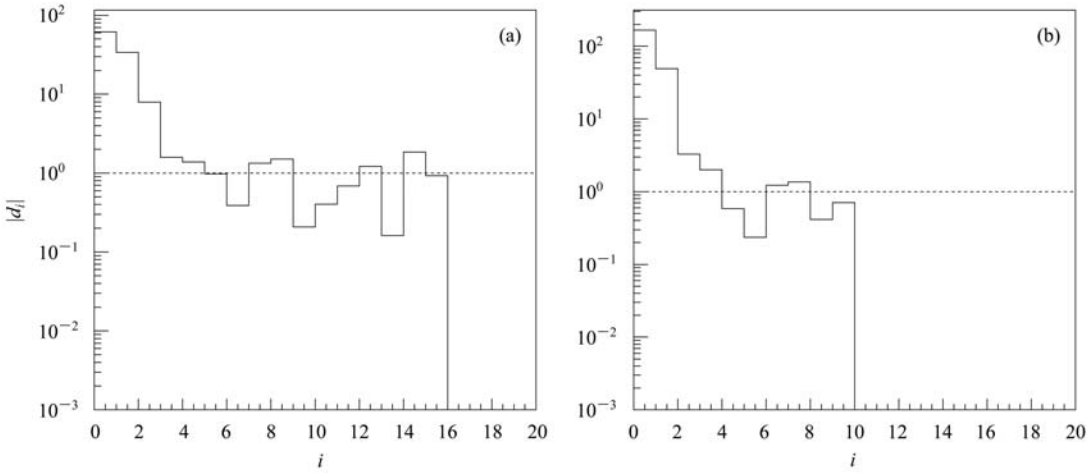

Fig. 4. Plots of $\lg|d_i|$ versus i for of Fe (a) and Pb (b) targets. The number of bins is 20 for both targets, while the number of measured events is 5000 for Fe and 30000 for Pb.

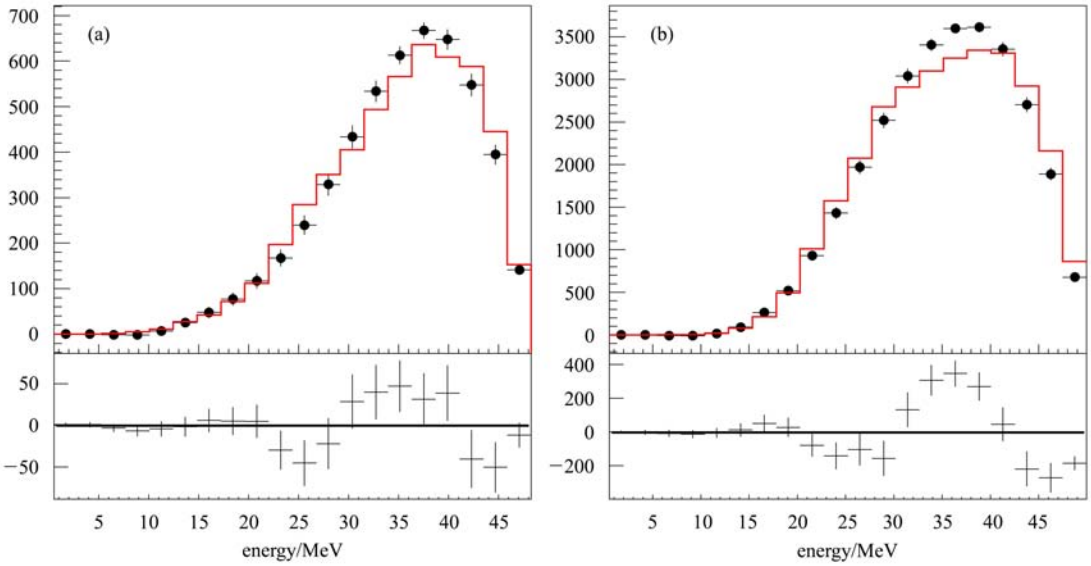

Fig. 5. Comparison between the unfolded and true energy spectra of the ν_e induced electrons, The target is Fe for (a) and Pb for (b). The number of bins is 20 for both targets, while the number of measured events is 5000 for Fe and 30000 for Pb. The solid red line in the upper plot is the true data (color only online), while the solid circles indicate the unfolded results. The lower plot shows the difference between unfolded results and true data.

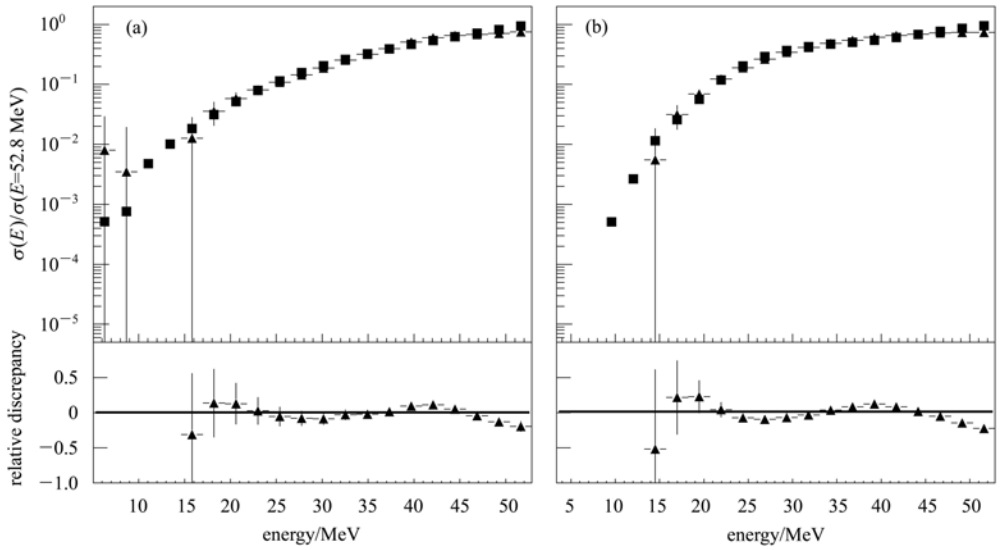

Fig. 6. Comparison between the measured and true differential cross sections of ν_e-Fe (a) and ν_e-Pb (b) scattering. The number of bins is 20 for both targets, while the number of measured events is 5000 for Fe and 30000 for Pb. $\sigma(E=52.8$ MeV) is 1.2×10^{-39} cm^2 for Fe and 1.3×10^{-38} cm^2 for Pb. The solid squares in the upper plot indicate the theoretical cross sections, while the solid triangles indicate the measured results. The lower plot shows the relative discrepancy between measured results and theoretical values.

parameter. It shows that for energy below 22 MeV the measured cross sections fluctuate significantly, and are therefore totally unreliable. While the discrepancies between 22 and 50 MeV are well controlled below 20%.

5 Conclusion

By using a Monte Carlo simulation, we studied the achievable accuracy of ν_e-nucleus scattering cross section measurement using an ideal segmented detector. Two different target materials, Fe and Pb, are investigated, since they are most relevant to the evolution of supernovae and experimental data of the cross section are still not available. The energy spectrum of the ν_e induced electron can be well reconstructed using the unfolding method, and therefore makes it feasible for the measurement of the differential cross section. For an Fe target, the cross sections between 20 and 50 MeV can be measured within 20% accuracy using 5000 events, the cross section below 20 MeV is however totally unreliable since the cross section is too small in this region. For a Pb target, the cross sections between 22 and 50 MeV can be measured within 20% accuracy using 30000 events, the cross sections below 22 MeV are not reliable due to low statistics.

We are grateful for the fruitful discussions with Dr. X. Zhu and Dr. Y. Lin for helpful discussions.

References

1 Bethe H A. Rev. Mod. Phys., 1990, **62**: 801–866
2 Totani T, Sato K. Astropart. Phys., 1995, **3**: 367–376
3 Kuzmin K S, Lyubushkin V V, Naumov V A. Eur. Phys. J. C, 2008, **54**: 517–538
4 Lazauskas R, Volpe C. Nucl. Phys. A, 2007, **792**: 219–228
5 Bodmann B et al. (KARMEN collaboration). Phys. Lett. B, 1992, **280**: 198–203
6 Auerbach L B et al. (LSND collaboration). Phys. Rev. C, 2001, **64**: 065501
7 Physics Division of the Oak Ridge National Laboratory. Proposal for a Neutrino Facility at the Spallation Neutron Source. 2005
8 Maschuw R. (KARMEN collaboration). Prog. Part. Nucl. Phys., 1998, **40**: 183–192
9 Armbruster B et al. (KARMEN collaboration). Phys. Lett. B, 1998, **423**: 15–20
10 Berger M J, Seltzer S M. Tables of Energy Losses and Ranges of Electrons and Positrons, NASA-SP-3012. Washington D C, 1964
11 Nakamura K et al. (Particle Data Group). J. Phys. G, 2010, **37**: 075021
12 http://geant4.cern.ch
13 Cowan G. Statistical Data Analysis. Oxford: Clarendon Press, 1998
14 Albert J et al. (MAGIC collaboration). Nucl. Instrum. Methods A, 2007, **583**: 494–506
15 Anykeev V B, Spiridonov A A, Zhigunov V P. Nucl. Instrum. Methods A, 1991, **303**: 350–369
16 Höcker A, Kartvelishvili V. Nucl. Instrum. Methods A, 1996, **372**: 469–481
17 http://root.cern.ch
18 http://hepunx.rl.ac.uk/ adye/software/unfold/RooUnfold.html